Atmospheric Research 124 (2013) 21–33

Contents lists available at SciVerse ScienceDirect

Atmospheric Research

journal homepage: www.elsevier.com/locate/atmos

Diurnal variability of stability indices observed using radiosonde observations over a tropical station: Comparison with microwave radiometer measurements

M. Venkat Ratnam [a,*], Y. Durga Santhi [b], M. Rajeevan [c], S. Vijaya Bhaskara Rao [b]

[a] National Atmospheric Research Laboratory, Gadanki, India
[b] Department of Physics, Sri Venkateswara University, Tirupati, India
[c] Ministry of Earth Sciences, New Delhi, India

ARTICLE INFO

Article history:
Received 16 May 2012
Received in revised form 18 December 2012
Accepted 18 December 2012
Available online 4 January 2013

Keywords:
Convection
CAPE
Radiosonde
Radiometer
Diurnal variation

ABSTRACT

Convection plays an important role in maintaining the thermodynamic structure of the atmosphere particularly in the tropical regions and it is often associated with clouds and precipitation. In the present study we report the diurnal variation of various stability indices observed using intensive radiosonde observations made during October 2010 to October 2011 over Indian tropical region, Gadanki (13.5°N, 79.2°E). Simultaneous co-located microwave radiometer (MWR) observations collected during April–October 2011 are used for comparison. Detailed comparison between these two independent techniques has been made which will be very much useful in assessing the data from MWR for Nowcasting. In general, MWR observations show warm (cold) bias in the temperature, except at 0.5 km, when compared to radiosonde observations below (above) 3–4 km, assuming latter as a standard technique. In case of water vapor, MWR observations show wet (dry) bias below (above) 2–3 km depending on the time. Nevertheless, very good comparison in several convection indices is noticed between the two different techniques, particularly in the trends though some differences are noticed in the amplitudes. For about 25% of time MWR is unable to estimate the Convective Available Potential Energy (CAPE) as equilibrium level is above the altitude that MWR can detect. Strong diurnal variation in CAPE and other thermodynamic parameters is noticed with maximum in the afternoon and minimum in the early morning hours in all the seasons except in winter over this tropical station.

1. Introduction

Convective activity plays a very important role in the tropics and it often leads to release of latent heat, formation of clouds and precipitation. Understanding this over the tropical regions is rather complex. It can be estimated by several indices like, lifted index (LI), level of free convection (LFC), equilibrium level (EL), Convective Available Potential Energy (CAPE), K index (KI), Cross Total (CT) index, Vertical Total (VT) index, Total Totals (TT) index, SHOWALTER index, S index (SI) etc., which have their own significance in measuring the stability of atmosphere. As specific examples, the K-index and its variants have been useful predictors of precipitation occurrence/amount and non-severe thunderstorm occurrence, while the CT, VT, TT, LI, and SHOWALTER indices (and variants thereof) have been valuable for predicting the severe weather.

Numerous studies have reported the seasonal and long-term variation of various atmospheric parameters like outgoing long wave radiation (OLR), sea surface temperature (SST), precipitable water and clouds, which may have direct or indirect effects on convective activity over different regions (Dai, 2000; Gettelman et al., 2002; Ueno and Aryal, 2007; Sapra et al., 2011). In the tropics, OLR

* Corresponding author. Tel.: +91 8585 272123; fax: +91 8585 272018.
E-mail address: vratnam@narl.gov.in (M.V. Ratnam).

0169-8095/$ – see front matter © 2012 Elsevier B.V. All rights reserved.
http://dx.doi.org/10.1016/j.atmosres.2012.12.007

variability is a good indication of convective activity associated with cumulus cloud development. It was shown that monthly scale OLR variability over the Himalayas is strongly affected by convection over the tropics in the months of December, March, and April (Ueno and Aryal, 2007). Dhaka et al. (2010) showed the relationship on seasonal, annual, and large scale variation in CAPE and solar scale temperature at 100 hPa pressure level using daily radiosonde data for a period of 1980–2006 over some stations in India.

A few studies deal with diurnal variation of convection indices over tropical regions. Nevertheless, the diurnal variation of convective activity over the tropical regions has been well documented (even though they are less in number) and provided the qualitative information by several researchers in many regions of the world (Mc Garry and Reed, 1977; Sato and Kimura, 2004; Ueno and Aryal, 2007; Johnson et al., 2010). Gray and Jacobson (1977) studied extensively the existence of large diurnal cycle of oceanic, tropical, deep cumulus convection and found that many stations recorded the rainfall 2–3 times in excess in the mornings compared to evening times. Mc Garry and Reed (1977) analyzed diurnal variations in convection and precipitation over West Africa and the tropical east Atlantic. They found that maximum convective activity in the eastern Atlantic occurred in the afternoon and suggested that continental influences may affect the diurnal cycle. Afternoon convective showers were more evident in the large-scale undisturbed periods when the diurnal SST cycle was strong, but the nocturnal convective systems and morning cumulus are more enhanced in the disturbed periods when more moisture was available (Sui et al., 1997).

Soden (2000) studied the variations in upper troposphere cloud and found that water vapor occurs in phase with changes in deep convection over land but nearly 12 h out of phase with over oceans. Monkam (2002) studied the distribution of the CAPE in northern Africa and the tropical Atlantic in summer in three different zones and showed that the rainfall and CAPE are very well correlated around the Inter tropical Convergence Zone (ITCZ) and towards some mountains, which indicates that each of these two parameters are influenced by ITCZ and orographic effects. Zhang (2003) studied the role of large scale forcing, surface fluxes and CIN in the diurnal variation of convection using the ARM SGP data and found a strong phase relationship with convection and also suggested that surface sensible and latent heat fluxes also generate CAPE, but are not released by convection. Sato and Kimura (2004) examined the diurnal cycle of convective instability around the central mountains in Japan during the warm season and found that abundant moisture accumulates over the mountainous areas in the afternoon and the specific humidity greatly increases at ~800 hPa level. The increase in specific humidity causes an increase of equivalent potential temperature near 800 hPa. As a result, the convective instability index increases over the plain at night. Narendra babu et al. (2009) also studied the diurnal time scales of global patterns of CAPE using one year of COSMIC/FORMOSAT-3 observations.

All these convective indices of the atmosphere need to be calculated using accurate data sets. The estimation of stability indices derived from thermo-dynamical parameters requires high accurate data sets of temperature and water vapor. Remote sensing of both temperature and water vapor is very important to predict severe weather and also to indicate the state of the atmosphere. Traditionally, atmospheric profiles of temperature, pressure, humidity, and winds can be derived from radiosonde observations to estimate thermodynamic parameters. Several studies (Westwater, 1997; Miloshevich, et al., 2001, 2004, 2006, 2009; Turner et al., 2003; Mattioli et al., 2007; Kottayil et al., 2011) have been reported to characterize and calibrate the radiosonde measurements and also compared with simultaneous measurements from reference instruments. These studies reveal the impact of bias between the different types of sensors. Miloshevich et al. (2009) compared the RS92 relative humidity with simultaneous WV measurements from cryogenic frost point hygrometer, atmospheric radiation measurement and Microwave Radiometer (MWR). Rowe et al. (2008) found the dry bias in Väisälä RS 90 radiosonde humidity profiles over Antarctica region and applied corrections between 650 and 200 mb. Recently Kottayil et al. (2011) applied corrections to the radiosonde observations and found better agreement between satellite and radiosonde measurements in the upper tropospheric humidity. Very recently Sanchez et al. (2012) reported a bias in the temperature and humidity measurements obtained by MWR and applied some bias correction using linear adjustment method, which significantly improves vertical temperature and water vapor density profile accuracy. However, radiosonde data are typically available at most twice a day, and thus they are not frequent enough to capture the rapid varying thermodynamic state of the atmosphere. In this connection, ground-based microwave radiometers (MWR), providing useful information on the temperature and humidity profiles, are alternative source of getting thermodynamic state of the atmosphere. These profiles are available continuously, nearly at intervals of every 5 min. It is already well proven (Chan, 2009; Chan and Hon, 2011; Cimini et al., 2011, 2012; Ware et al., 2010; Herzegh et al., 2004) that these MWR are able to provide very useful data in the Nowcasting of convective weather, which is also our main motivation. Knupp et al. (2009) and Vandenberghe and Ware (2002) also showed the capabilities of MWR in operational forecasting during dynamic weather conditions. Nevertheless, it is essential to assess the quality of observations from these instruments at various regions before using it for Nowcasting.

In this present study, an attempt has been made first to find out the biases in the temperature and water vapor measurements between radiosonde and MWR at different timings. For this, we made use of intensive radiosonde launchings conducted every 3 h for 3 days in each month. Second, we determined the percentage of time MWR provides inadequate information on parameters including EL and CAPE. Third, detailed comparison of all the stability indices have been made using simultaneous radiosonde and MWR observations. Fourth, percentage stability index differences between the two independent techniques were determined. Finally, diurnal variations of some of the convection indices have been reported. We believe that this work will be useful to assess the MWR observations for predicting or diagnosing particular atmospheric phenomena in the absence of radiosonde observations.

2. Data

2.1. Radiosonde measurements

High-resolution radiosonde (Väisälä RS-80, RS-92, Meisei RS-01GII) balloons launched daily over Gadanki (13.5°N, 79.2°E) during the period of April 2006 to December 2011 is used to study the atmospheric stability parameters. Gadanki is a tropical rural station surrounded by a complex terrain environment and it is located about 120 km northwest of Chennai (Madras) on the east coast of the southern peninsula. The location of this station is depicted in Fig. 1 along with topography. The local topography is rather complex, with a number of small hills with a maximum height of 200–400 m, and the station is at a height of 375 m above mean sea level and an irregular mix of agriculture and small population centers. Most of these radiosondes were launched around 1730 h Local Time, LT (LT = UT + 0530 h). In addition, radiosondes were launched every 3 h for 72 h in each month since October 2010 as a part of Climate and Weather of Sun Earth Systems (CAWSES) India Phase II program. The dates and timings at which radiosonde were launched is shown in Fig. 2. All the atmospheric parameters like temperature (T), relative humidity (RH) and horizontal wind are obtained with a height resolution of 25–30 m (sampled at 5-s intervals) from RS-80 type (April 2006 to March 2007) and 10 m (sampled at 2-s intervals) from RS-92 (from 17 July 2006 to 31 August 2006) and Meisei (May 2007 to December 2011). Later, the entire data set has been interpolated to 100 m so as to remove outliers arising from random motions of the balloon.

2.2. MWR measurements

Passive instruments like MWR, which is less expensive and has high temporal resolution than other relevant techniques (e.g., radiosonde, air planes), can be used to operate in any weather conditions. A multi wavelength MWR (MP-3086A, USA) has been installed at Gadanki in March 2011. This MWR consists of 35 calibrated channels in two radio frequency subsystems. The temperature (water vapor) profiling subsystem utilizes sky brightness temperature observations at selected frequencies between 51 (22) and 59 (30) GHz. The radiometer produces profiles at 50 m resolution up to 0.5 km, 100 m resolution from 0.5 km to 2 km and 250 m from 2 km to 10 km. However we interpolated to 100 m resolution for comparison with radiosonde observations. According to Knupp et al. (2009) and Chan (2009), retrieval of temperature and humidity profiles from the MWR is usually done by neural network methods based on historical radiosonde data, using a radiative transfer model to simulate the observations of a MWR. In this study, the neural network was trained by a high-resolution radiosonde dataset collected at Gadanki since April 2006. Only zenith mode measurements by the MWR are used to retrieve the temperature and humidity profiles up to ~10 km above ground for the period of six months during April–October 2011 and the dates are shown in Fig. 2. These observations are compared with the intensive radiosonde launched for every 3 h for 3 days in each month. The height and the pressure are related using hydrostatic approximation. These profiles are then employed to determine the thermodynamic parameters in a severe weather conditions. It is well known that the CAPE is a potential indicator of the convective activity in the atmosphere. As the MWR data is limited up to ~10 km corresponding to ~300 hPa, it is not possible to get the EL always when it occurs beyond the 300 hPa to calculate the CAPE. For this reason, most unstable CAPE (MUCAPE) is often calculated using the virtual temperature of the most unstable parcel in the lowest 300 hPa, in order to determine the lower tropospheric instability.

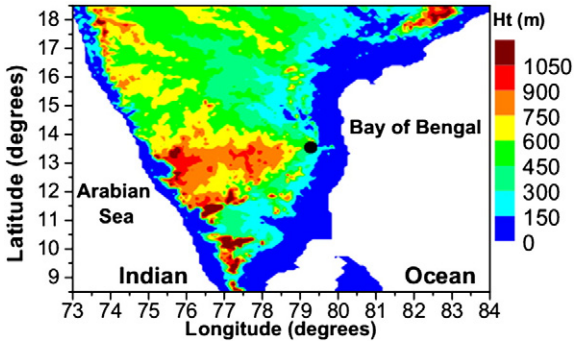

Fig. 1. Topography of Indian sub-continent. Location of Gadanki is shown with filled circle.

3. Methodology

In this section we briefly mention the calculation procedure followed for estimating various stability indices. CAPE is a measure of amount of energy that is available during convection and is often calculated by integrating vertically the local buoyancy of the parcel from the level of free convection (LFC) to equilibrium level (EL).

$$CAPE = \int_{EL}^{LFC} g\left(\frac{Tv_{parcel} - Tv_{env}}{Tv_{env}}\right) dz \quad (1)$$

Where, LFC and EL are respectively the heights of Level of Free Convection and Equilibrium Level. Tv_{parcel} is virtual temperature of the parcel and Tv_{envs} is the virtual temperature of the environment, g is acceleration due to gravity. The LFC is the height above LCL, where the parcel temperature is greater than environment temperature and it is found by raising a parcel moist adiabatically. EL or Level of Neutral Buoyancy (LNB) is the height above the LFC where the parcel temperature is less than the environment temperature or becomes equal. This means the unstable air is now stable at EL where the convection ceases. If the environment is stable and there is no LFC, there is obviously no EL.

A typical example showing the thermodynamic sounding diagram obtained from radiosonde observations obtained on 19 August 2011 at 1700 h LT over Gadanki is shown in Fig. 3. Environment temperature, parcel temperature, LCL, LFC and EL are also indicated in the figure. On the evening of 19 August 2011, thunderstorm developed over Gadanki region during 1400 h to 1600 h LT. These thunderstorms eventually formed a mesoscale convective system with a low level jet over Gadanki and surrounding regions and transports moisture towards north. These storms created heavy rainfall across the region during the early morning hours on 20 August 2011 before moving off to south. During this period, estimated CAPE value is 1517 J/kg at 1430 h and increased to 1722 J/kg by 1730 h LT.

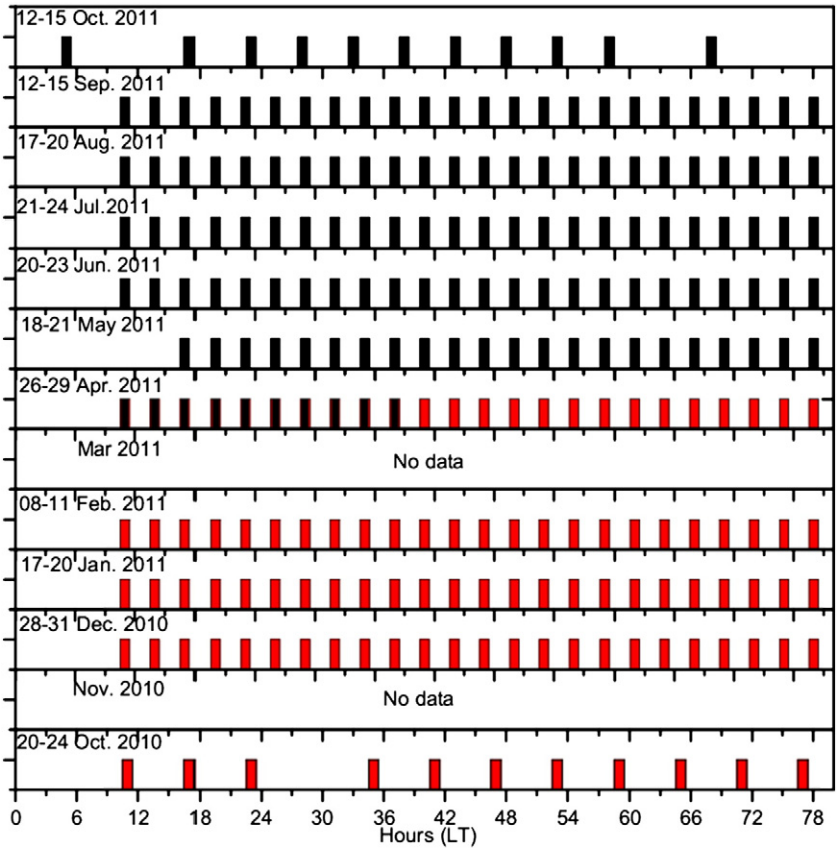

Fig. 2. Hours at which radiosonde launchings are made during the 3 day period in each month from October 2010 to October 2011. The hours at which the data available from co-located MWR during April to October 2011 is shown in black bars.

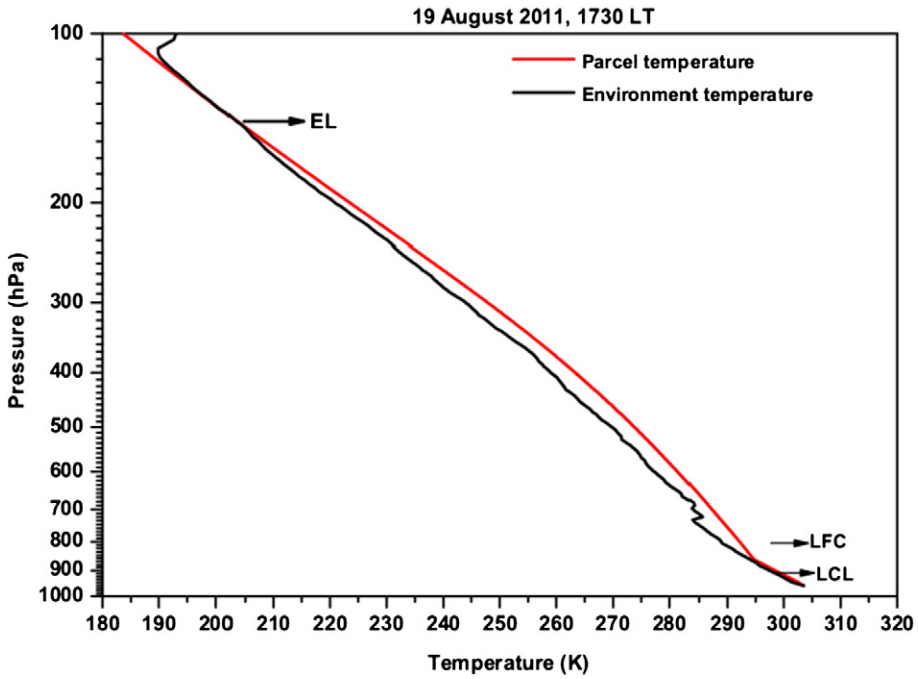

Fig. 3. Typical example showing the thermodynamic sounding diagram using radiosonde observations obtained on 19 August 2011 at 1730 h LT over Gadanki. Environment temperature, parcel temperature, LCL, LFC and EL are also indicated.

The LCL, LFC, EL are estimated to be 883.9 hPa, 859.3 hPa, and 140.7 hPa, respectively, which are also shown in Fig. 3. On a thermodynamic diagram the LCL is located at the point of intersection of the saturation mixing ratio curve corresponding to the parcel's initial dew point temperature and the dry-adiabatic representing the parcel's initial temperature. Various stability indices, for which analysis procedure is mentioned below, estimated for this typical example is provided in Table 1.

3.1. Most unstable CAPE (MUCAPE)

MUCAPE is a measure of instability in the troposphere. This value represents the total amount of potential energy available to the most unstable parcel of air found where the environment temperature reaches to −20 °C of the atmosphere while being lifted to its LFC. No parcel entrainment is considered. The MUCAPE for the example shown in Fig. 3 is 279.93 J/kg.

3.2. Lifted index (LI)

The LI is the temperature difference between an air parcel lifted adiabatically Tp (p) and the temperature of the environment Te (p) at a given pressure in the troposphere usually at 500 mb. The LI for the example shown in Fig. 3 is −3.95.

3.3. Cross total (CT) index

The CT index is the difference between the dew point temperature (T_d) at 850 hPa and temperature at 500 hPa which is given as:

$$CT = T_{d-850hPa} - T_{500hPa} \quad (2)$$

Since the mixing ratio can be expressed in terms of dew-point temperature at a certain pressure level, the CT index (Miller, 1967) increases with a combination of moisture at low levels (850 hPa) and relatively cold air at upper levels (500 hPa). The CT index for the example shown in Fig. 3 is 18.73.

Table 1
Various stability indices estimated using the radiosonde observations obtained on 19 August 2011 at 1730 h LT over Gadanki.

S. no.	Parameter	Value
1.	CAPE (J/kg)	1722.37
2.	MUCAPE (J/kg)	279.93
3.	Lifted condensation level	883.45
4.	Temperature at LCL	294.67
5.	Level of free convection	859.65
6.	Equilibrium level	140.7
7.	Lifted index	−3.95
8.	Cross total index	18.7389
9.	Vertical total index	23.238
10.	Total total index	41.9769
11.	K-Index	35.442
12.	Show ALTER index	−14.7206
13.	S-Index	25.8334

3.4. Vertical total (VT) index

The VT index (Miller, 1967) does not consider moisture and only assesses conditional instability between 850 and 500 hPa. Since the 850–500 hPa layer thickness increases with increasing temperature, the actual lapse rate will be underestimated in summer and overestimated in winter. The VT index for the example shown in Fig. 3 is 23.24.

$$VT = T_{850hPa} - T_{500hPa} \quad (3)$$

3.5. Total total (TT) index

TT index (Miller, 1967) is a commonly used convective index in many parts of the world, but was originally designed for application in the U.S. (Peppler and Lamb, 1989). It fails to consider latent instability below 850 hPa. The TT index for the example shown in Fig. 3 is 41.98.

$$TT = CT + VT \quad (4)$$

3.6. K-Index (KI)

George (1960) developed the K-Index for forecasting air mass thunderstorms. This index increases with decreasing static stability between 850 and 500 hPa, increasing moisture at 850 hPa, and increasing relative humidity at 700 hPa. The K-Index for the example shown in Fig. 3 is 35.44.

$$KI = (T_{850hPa} - T_{500hPa}) + T_{d-850hPa} - (T_{700hPa} - T_{d-700hPa}) \quad (5)$$

3.7. SHOWALTER Index (SAI)

This index is defined as the difference between the observed temperature at 500 hPa (T_{500}) and the temperature of an air parcel after it has been lifted pseudoadiabatically to 500 hPa from 850 hPa.

3.8. S-Index (SI)

$$SHOW = T_{500hPa} - T'_{850hPa \rightarrow 500hPa} \quad (6)$$

$$SI = TT - (T_{700hPa} - T_{d-700hPa}) - A \quad (7)$$

Where A is defined as follows: If VT > 25, then A = 0; if VT 22 and 25, then A = 2; if VT < 22, then A = 6. TT and VT are defined later in this section. The SHOW and S index for the example shown in Fig. 3 is −14.72 and 25.83, respectively.

4. Results and discussion

4.1. Diurnal variation of temperature and specific humidity

Fig. 4 shows the diurnal variation of temperature (Fig. 4a) and specific humidity (Fig. 4b) observed during 17–19 August 2011 over Gadanki region from the radiosondes launched at three hour intervals. The temperature (Fig. 4c) and specific humidity (Fig. 4d) obtained from MWR is also shown

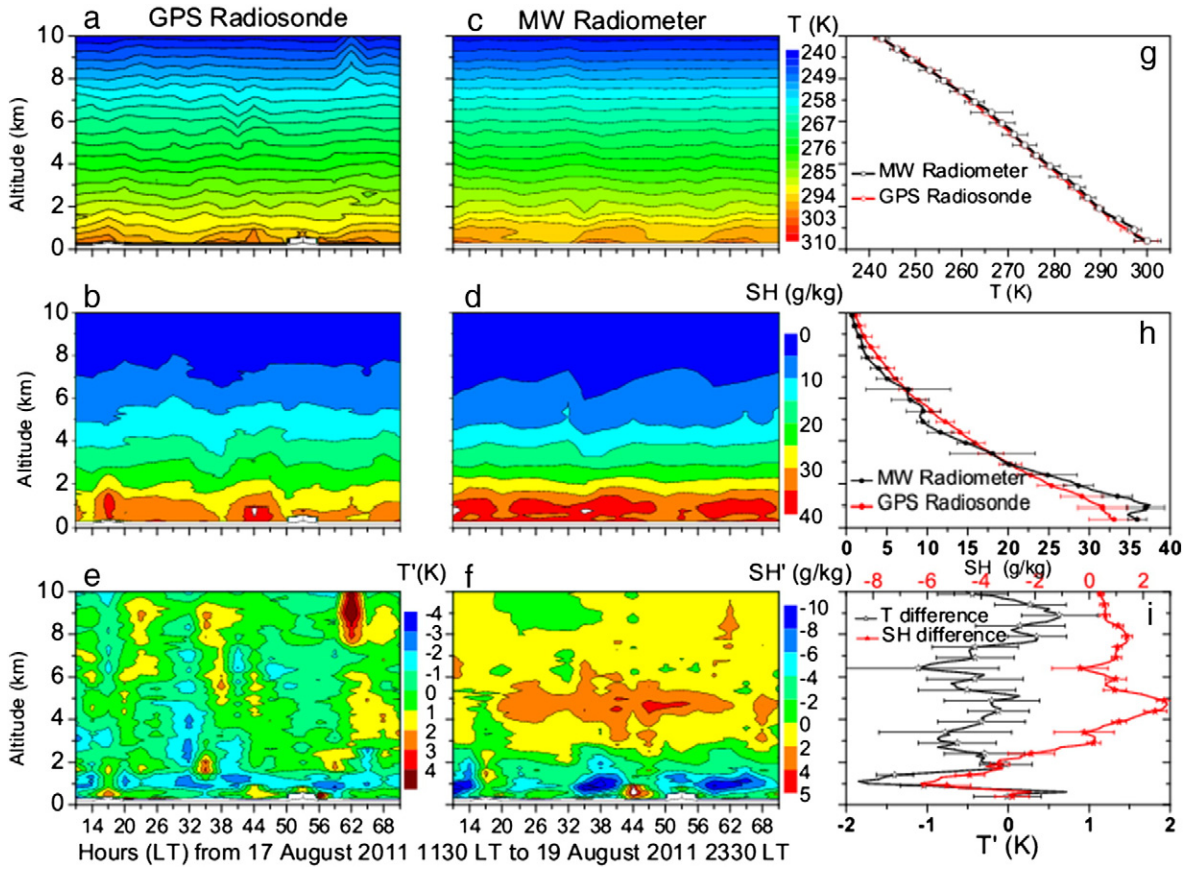

Fig. 4. Time-height plots of the (a) temperature and (b) specific humidity observed by radiosonde during 17–19 August 2011. (c) and (d) same as (a) and (b) but observed by MWR. (e) and (f) same as (a) and (b) but difference between radiosonde and MWR observed temperature and specific humidity, respectively. Mean profiles along with standard deviations in (g) temperature and (h) specific humidity averaged during 17–19 August 2011. (i) Mean difference and standard deviations between radiosonde and MWR.

for comparison. In general the temperature decreases with altitude and the maximum temperatures are found near the surface with minor irregularities. High specific humidity values which are favorable for more convective activity are observed near to the surface and up to 1 km in both the measurements.

The mean and standard deviation profiles of temperature and specific humidity obtained while averaging the observations during 17–19 August 2011 from both the instruments are shown in Fig. 4g and h, respectively. Note that mean profile of temperature observed by MWR falls within the standard deviation of temperature of radiosonde showing the consistency in the observations. However, specific humidity from MWR shows higher values in the lowest 3 km and slightly lower values above it. Thus, MWR shows a wet bias with respect to the radiosonde in the lower levels. More detailed comparison between these two different techniques is shown in the following sub-section. The difference in temperature and specific humidity obtained during the above mentioned period from radiosonde and MWR has been shown in Fig. 4e and f, respectively. Except in first few meters above the ground and above 8 km, for temperature there is a warm bias in MWR and is smaller than 2 K. It is interesting to note strong dry bias in MWR between 4 and 6 km irrespective of the time of the day. Mean difference and standard deviation of temperature and specific humidity between the both instruments are also shown in Fig. 4i. For temperature the standard deviations increase with height but they are smaller than 2 K. For Specific humidity there is a wet bias in MWR below 3 km, dry bias between 3 and 5.5 km and negligible bias above 5.5 km. The standard deviation again increases with altitude but is mostly within the 2 g/kg.

4.2. Comparison between radiosonde with MWR observations at different times

Extensive comparison of the temperature and specific humidity profiles between the radiosonde and MWR are performed in order to see the differences in the measurements between the two instruments. Fig. 5a–d shows the temperature differences between the radiosonde and MWR obtained during April–October 2011 from the special campaign conducted over Gadanki at 00, 06, 12, and 18 UT, respectively. The number of simultaneous profiles used for this comparison is also shown in the figure. MWR observations are averaged for about half an hour to match the flight time of radiosonde to reach an approximate altitude of 10 km. The warm (cold) bias (radiosonde minus MWR) in temperature in MWR is clearly observed below (above) the 4 km altitude at 00 and 06 UT, assuming radiosonde as standard technique. However, this altitude

changes to 3.5 km around 12 UT and 18 UT. The maximum warm bias of ~2 K in temperature in MWR is found around 1 km during 00 UT and 18 UT, however, around 2.5 km in the 12 UT. Interestingly, large standard deviations in the temperature differences between the two instruments are noticed around 00 UT. Cold bias in MWR around 5–6 km is more during 06 UT and 12 UT when compared to other timings. It is also interesting to note a small cold bias consistently appearing at all the timings around 0.5 km.

Fig. 5e–h shows the specific humidity biases between the radiosonde and MWR obtained during April–October 2011 over Gadanki at 00, 06, 12, and 18 UT, respectively. A large wet (dry) bias of 6–8 g/kg in the specific humidity below (above) 3 km is noticed at 00 UT and 06 UT between the radiosonde and MWR. This altitude changes to 2 km and 2.5 km at 12 UT and 18 UT, respectively. Highest wet bias is observed around 06 UT followed by 12 UT and 18 UT with minimum difference at 00 UT. Above the altitude of 2–3 km, there is a slight dry bias except around 5–6 km where wet bias is again noticed. Note that the lesser the amounts of water vapor in the air, greater the amount of heat lost to space by the Earth's long-wave radiation. Specific humidity profiles from the MWR tend to show an elevated, moist layer at 1 to 2 km. Difference in specific humidity shows large variations in the lower and middle troposphere i.e. below 5 km during all hours, whereas in the upper troposphere i.e., above 6 km the difference is almost negligible.

It is clear that MWR shows warm and wet bias in the temperature and specific humidity, respectively, at almost all the times over this station in the lower troposphere similar to that observed by Chan (2009) over Hong Kong. We cannot attribute this difference is due to spatial separation as they are co-located unlike reported by Chan (2009). One possible explanation is that this could due to the separation of space as the radiosonde drifts along with the wind whereas MWR looks always the same space. However, note that maximum separation between the two below 3 km never exceeded 5 km over this location in any season. Thus, more or less same atmosphere is being probed by both the instruments. It is also worth to note that Chan (2009) found a warm bias from surface to 1.4 km whereas in our case it is up to 3–4 km with stronger biases. He found negative humidity biases in the MWR in the first 1 km whereas we found positive biases. Regarding the bias in the water vapor profiles, note that several investigators (Cady-Pereira et al., 2008; Rowe et al., 2008) have shown that the daytime water vapor profiles measured by the radiosonde (Väisälä) have significant dry bias due to the solar heating of the humidity sensor. When correction algorithm was applied to the radiosonde observations, there was a better agreement (Westwater et al., 2003).

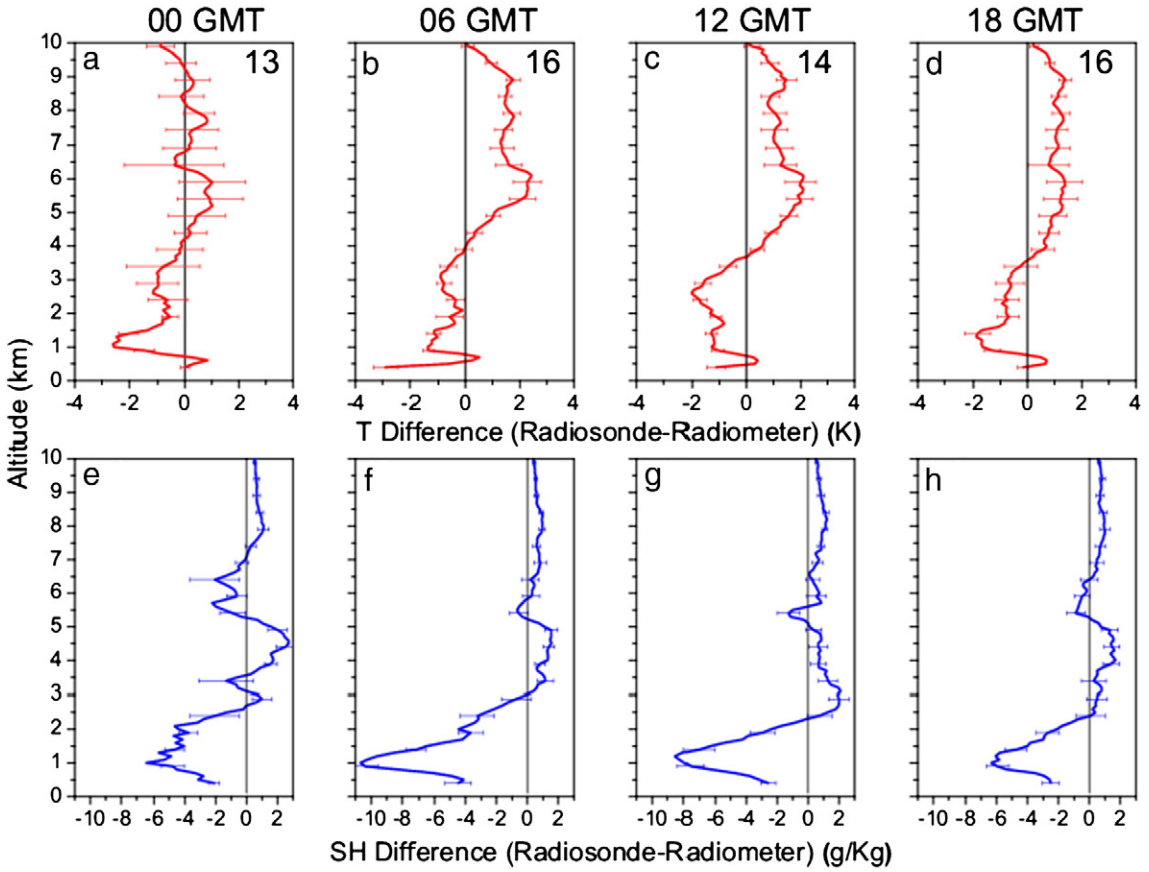

Fig. 5. Profiles of mean differences along with the standard deviations in the observed temperature (top panels) and specific humidity (bottom panels) between radiosonde and MWR obtained for 00 UT, 06 UT, 12 UT and 18 UT. The total number of profiles used is also mentioned in the top panels.

However, in the present study we see the differences between the two irrespective of the day and night times. Thus, other reasons need to be explored for explaining the observed discrepancy between the two techniques and it is out of scope of the present study.

4.3. Percentage occurrence of LFC and EL at different pressure levels

It is well known and as already mentioned above, CAPE is a measure of amount of energy that is available during convection and is calculated by integrating vertically the local buoyancy of the parcel from the LFC to equilibrium level EL. Since continuous measurements of LFC and EL are not available from routine radiosonde measurements, we need to depend heavily on the continuous measurements available from MWR. As also mentioned earlier, there are some limitations in the MWR observations at higher altitudes. At the best, they can provide measurements up to an altitude of 10 km (~300 hPa). Therefore, it is necessary to find out how much percentage of time EL is above this altitude. Radiosonde observations available for more than 5 years from this location have been utilized for this purpose. Fig. 6 shows the percentage occurrence of LFC and EL at different pressure levels over Gadanki region during the period Apr. 2006–Dec. 2011 observed in different seasons. The total number of profiles used are 1623 out of which 369, 468, 413, and 373 falls under pre-monsoon (MAM), monsoon (JJA), post-monsoon (SON), and winter (DJF), respectively. The number of profiles in which the EL crosses the 300 hPa is also mentioned in the Fig. 6. In general, for about 25% of time the EL is above 300 hPa revealing that MWR observations are not good enough to estimate the CAPE over Gadanki region. If we see season wise, EL is above 300 hPa for about 24.9%, 39.5%, 35.1% and 4% during pre-monsoon, monsoon, post-monsoon and winter, respectively. LFC values are mostly (75%) in between 900 and 700 hPa in all most of all the seasons except in winter where it lies in between 1000 and 800 hPa and very little time it exceeds 500 hPa. Note that all these estimations are made for the data obtained at 1730 h LT and the statistics differ when we consider other timings.

4.4. Diurnal variation of atmospheric stability indices

To demonstrate the diurnal cycle of stability indices over Gadanki, the initial parcel level has been taken as 957 hPa, as Gadanki is located at the altitude of 375 m from the mean sea level. Diurnal variation observed in CAPE, MUCAPE, pressure at LCL, LFC, CT index, VT index, TT index, K index, SHOWALTER index and S index observed using radiosonde data launched for every 3 h for 3 days during 17–19 August 2011 is shown in Fig. 7. Strong diurnal variation in all the stability indices can be noticed with maximum during 1400 h–1700 h LT where the maximum convection is expected to took place at this station and minimum during mid-night hours to early morning hours. Strong day-to-day variations in all the stability indices can be noticed within afternoon hours in the three days. The pressure at LCL (Fig. 7c) is about 850–870 hPa during afternoon hours which is very close to the earth's surface. The pressure at LFC (Fig. 7d) is about 770 hPa where the difference between LFC and LCL is very low suggesting that the convection starts very close to the earth's surface. The pressure at EL (Fig. 7e) is about 160 hPa and LI value is very less at 1400 h LT coinciding with high CAPE values (Fig. 7a). The K index (Fig. 7j) and CT index (Fig. 7g) value increases from noon time representing the unstable atmosphere conditions. The VT (Fig. 7h) and TT (Fig. 7i) indices are also very high at afternoon hours providing emphasis to maximum CAPE values, with respective to SHOW (Fig. 7k) and SI (Fig. 7l) values.

Diurnal variation observed in all the stability indices estimated using MWR during the same period is also superimposed in the respective panels in Fig. 7. Very good

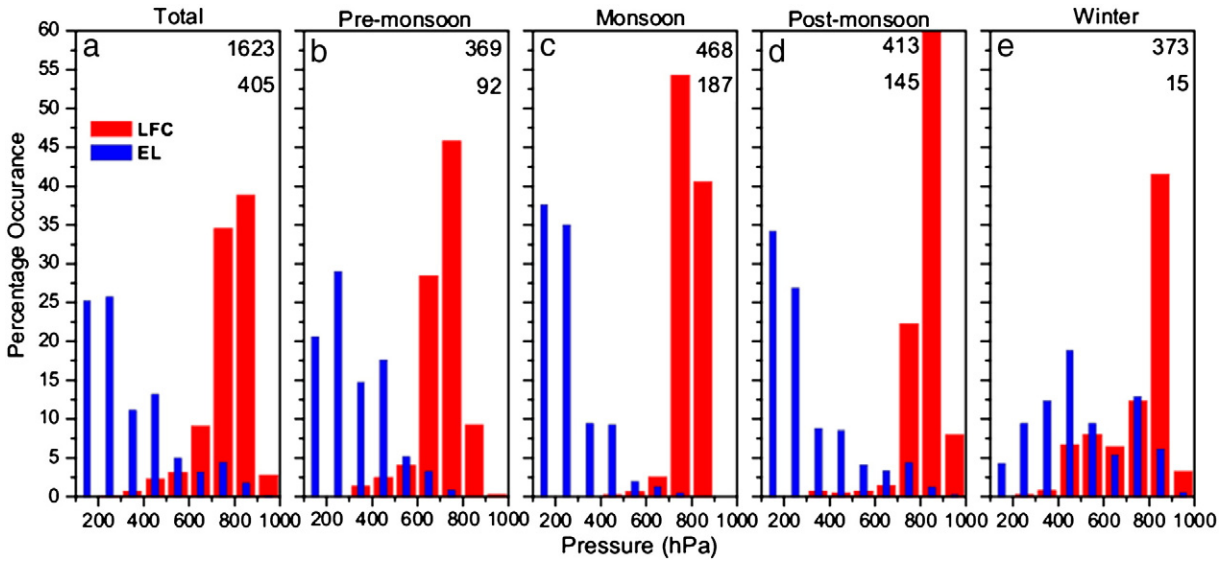

Fig. 6. Histograms showing the percentage occurrence of LFC and EL at different pressure levels observed during (a) Total period (2006–2010) (b) pre-monsoon, (c) monsoon, (d) post-monsoon and (e) winter seasons over Gadanki region. The total number of profiles and the number of profiles crossing the EL above 300 hPa is also mentioned in the respective panels.

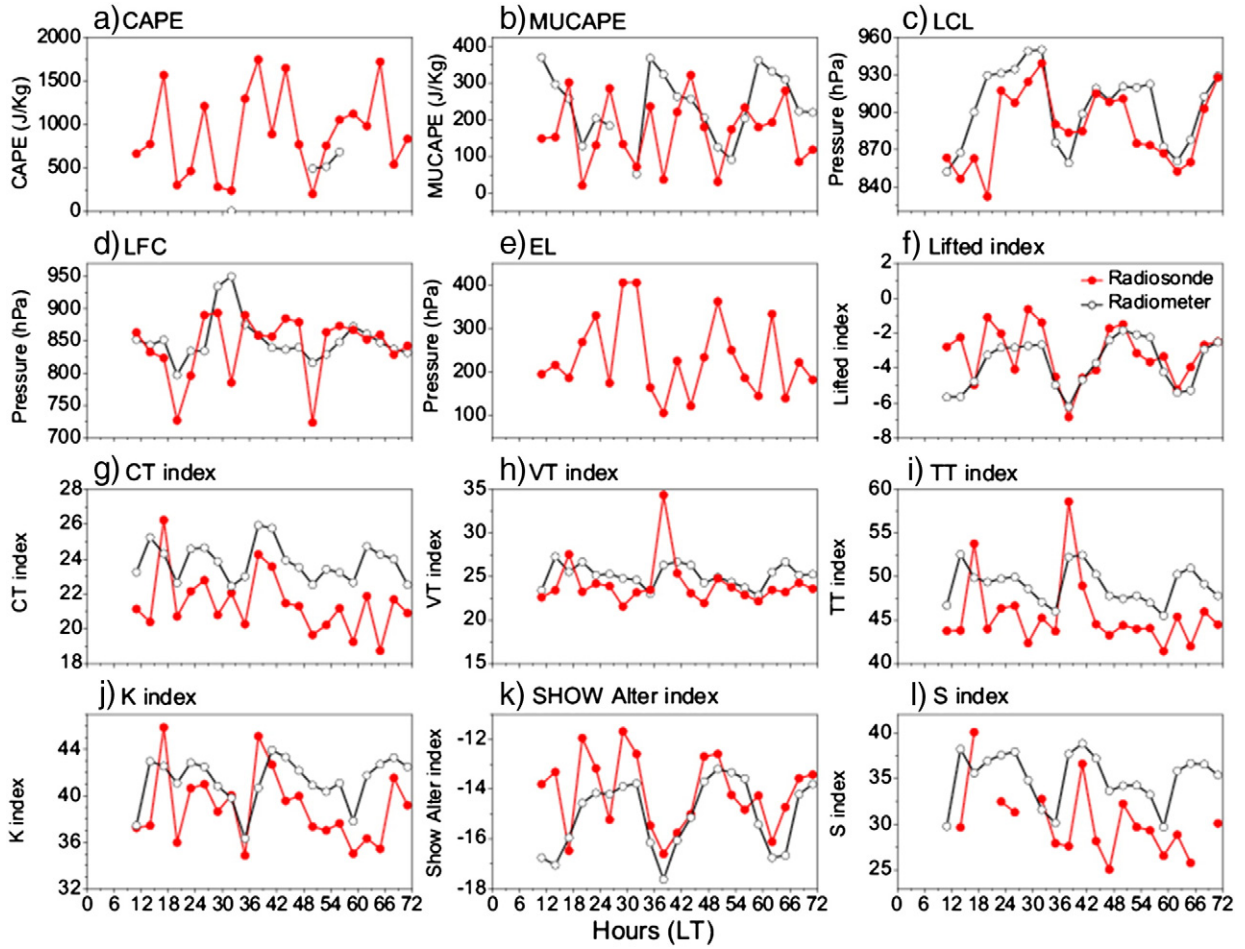

Fig. 7. Diurnal variation of (a) CAPE, (b) MUCAPE, (c) LCL, (d) LFC, (e) EL, (f) LI, (g) CT index, (h) VT index, (i) TT index, (j) K index, (k) SHOW ALTER index, and (l) S index obtained using 3-hourly radiosonde observations (red line) and MWR (black line) during 17–19 August 2011. (For interpretation of the references to color in this figure legend, the reader is referred to the web version of this article.)

comparison between the two techniques can be noticed, in general, particularly in the trends though some difference exists in the amplitudes. Note that CAPE values are missing (except during night times of 19 August 2011) due to non-availability of the information related to EL (Fig .7e) most of the time in MWR observations. In this connection MUCAPE (Fig. 7b) is often calculated to indicate the stability of atmosphere and it is defined as where the parcel lifted adiabatically from LFC to −20 °C (at environment temperature). Reasonably good comparison can be seen in MUCAPE between the radiosonde and MWR estimated values. The temperature at LCL from MWR is in the range of 295–296 K, whereas it is observed to be in the range of 290–298 K in radiosonde observations (figure not shown).

The more negative value of LI (Fig. 7f) represents the more unstable atmosphere leading to higher convective activity. LI values are more negative ranging between −4 and −8 revealing that the convective activity is more and there is a probability of occurrence of thunderstorms. It was shown that the best LI predicted instability regions in the afternoon that were associated thunderstorm activity. The K-index (Fig. 7j) limits of ≤+25 and ≤+30 were most related to the occurrence of measurable rainfall, particularly during 1400–1700 h LT. The SHOWALTER index was found to be a fairly good indicator of rain conditions and good agreement with MWR observations. In general, MWR estimated values are consistently higher in K-index, CT index, VT index, TT index and SI index. These differences between the two are mainly due to the inherent differences observed in the temperature and specific humidity which is mentioned in Section 4.2. Although these indices indicate the stability of the atmosphere focus is given to the K-index so as to compare results with those already reported. K-index is commonly used to estimate the occurrence of thunderstorms. During afternoon hours K-index values rise steadily and exceed 40 during evening hours which indicates the atmosphere is more unstable and began to fall gradually during morning hours. Similar features are observed by Chan (2009) during lightning activity associated with rain bands in the summer monsoon over Southern China.

4.5. Percentage error of atmospheric stability indices

The percentage differences (error) observed in all the stability indices between the radiosonde and the MWR is further calculated for the period April–October 2011 to assess how much error occurs if one depends only on MWR observations over this location and is shown in Fig. 8. Though MUCAPE is

mostly preferred from MWR as much of the time EL is above 300 hPa, however, the maximum difference between the radiosonde and MWR can go as high as 60% during morning hours even in this parameter. Interestingly during peak convection time (1400–1700 h LT) the error between the two estimates are minimum. On the other hand, percentage difference in LFC and LCL between the radiosonde and MWR show minimum. In case of LI, 50–80% difference can be noticed and the difference reduces during evening hours. In contrast to this, CT, VT, TT, K, SHOWALTER and SI values show maximum differences during afternoon hours of 1100–1400 h LT and minimum differences during night times.

4.6. Diurnal variation observed in CAPE, MUCAPE and LI

Fig. 9 depicts the diurnal variation of convection indices observed during different seasons. As mentioned earlier from October 2010 to October 2011 we have launched radiosondes every 3 h for 3 days every month except during November 2010. Fig. 9a–d shows the diurnal variation of CAPE observed during different seasons and vertical bars shows the standard deviations obtained while averaging over a season. Large diurnal variation can be observed in all the seasons except in winter. Large CAPE values during 1400–1800 h LT, in general can be noticed. The magnitude of the CAPE is high during pre-monsoon season when compared to the monsoon and post-monsoon seasons. During winter season the CAPE values are almost negligible which represents the fair weather. Similar features are seen in MUCAPE also during all seasons which are depicted in Fig. 9e–h. Interestingly, the values in all the seasons are more or less same except in winter. As mentioned earlier, LI is used to determine the stability of the lower half of the troposphere and the diurnal variation of LI is shown in Fig. 9i–l. The more negative value of LI represents the more unstable atmosphere resulting to more convective activity. During pre-monsoon season, LI values are more negative, ranging between −3 to −5 indicates strong convective activity and there is probability to occurrence of thunderstorms. During monsoon season the magnitude of LI values are less compared to the pre- monsoon months, where the thunder storm activity is less, when the monsoon is well established. The less LI values found during 1400–1600 h LT in

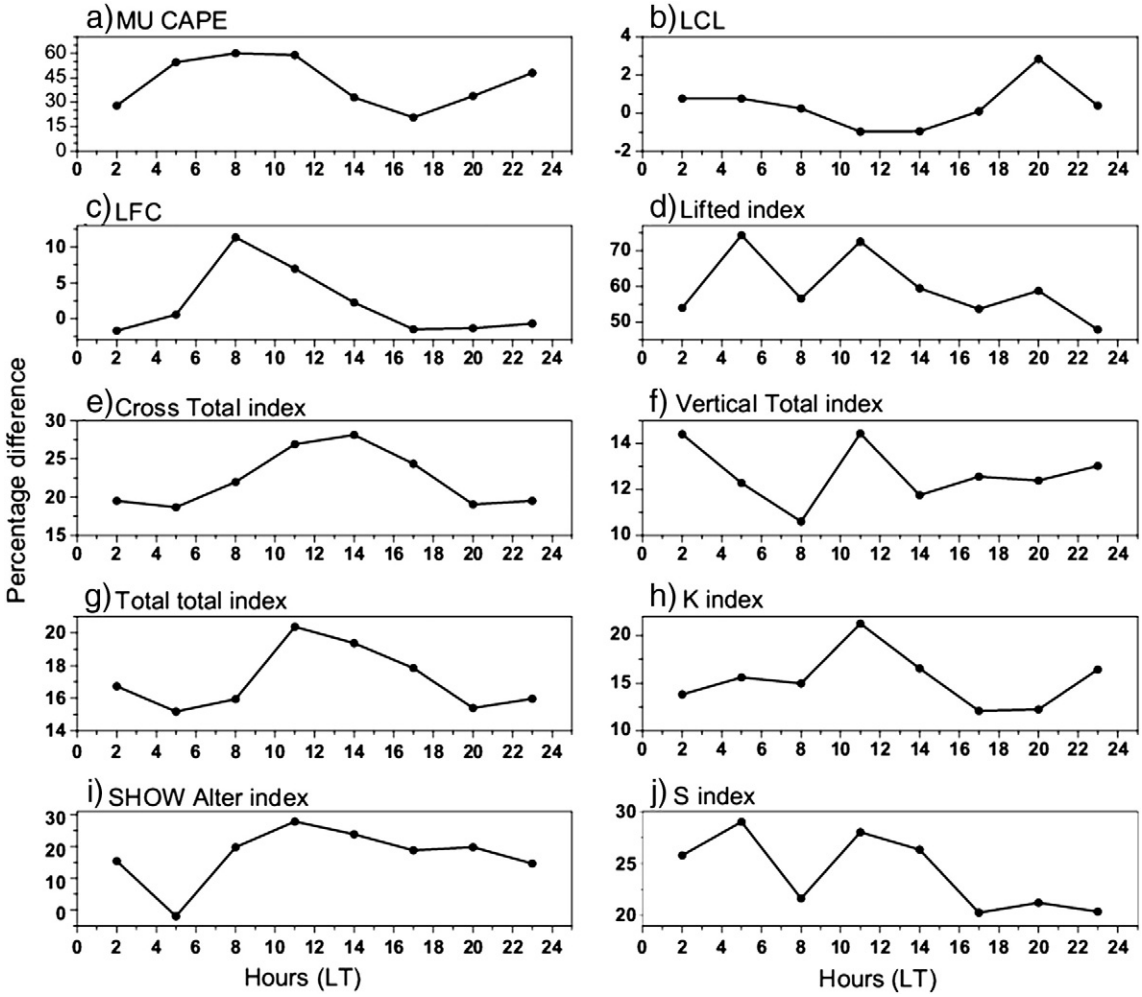

Fig. 8. Percentage difference between the radiosonde and MWR observed in (a) MUCAPE, (b) LCL, (c) LFC, (d) LI, (e) CT index, (f) VT index, (g) TT index, (h) K index, (i) SHOWALTER index, and (j) S index obtained using 3-hourly radiosonde observations during April–October 2011 and simultaneous MWR measurements.

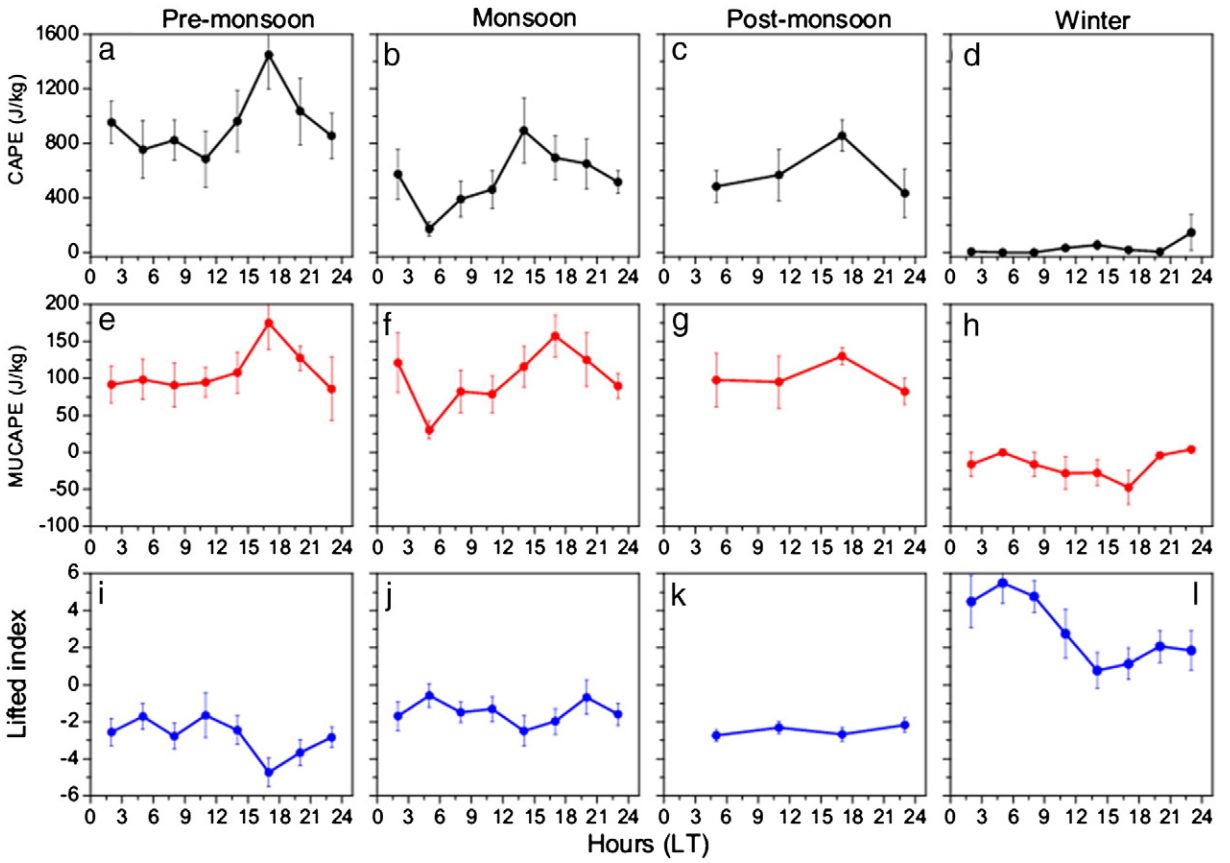

Fig. 9. Diurnal variation observed in CAPE (top panels), MUCAPE (middle panels) and LI (bottom panels) obtained from 3-hourly radiosonde observations during different seasons during 2010–2011. The vertical bars show the standard deviations obtained while averaging over respective seasons.

all seasons except winter season gives emphasis to high CAPE values. Fair weather conditions prevailed over Gadanki region, where the LI values are positive during winter season. Note that we have provided information on diurnal variation of few convection indices only which are most important.

5. Summary and conclusions

Several studies (Chan, 2009; Knupp et al., 2009) had shown that MWR provides useful data for Nowcasting the intense convective activity. In the present study, it is shown that the atmospheric stability indices derived from the temperature and humidity profiles obtained from three hourly launched radiosonde and MWR observations provide the valuable information for predicting the severe weather. In general, getting temperature and water vapor information from radiosonde observations for complete diurnal cycle are expensive. On other hand, MWR provides continuous observations of both temperature and water vapor in all weather conditions with few limitations (particularly upper limit in the altitude). In this present study, it is tested how good MWR observations can be utilized to estimate stability indices over a tropical station Gadanki assuming radiosonde as standard technique. As a first step towards this, an extensive comparison of temperature and specific humidity between the two different techniques has been made using 3 hourly radiosonde observations obtained for 3 days in each month during October 2010 to October 2011. The main findings are summarized in the following:

1. The warm (cold) bias between radiosonde and MWR in temperature is clearly observed below (above) 3–4 km depending upon the time. A large wet (dry) bias of 6–8 g/kg in the specific humidity below (above, except around 5–6 km) 2–3 km is noticed between the radiosonde and MWR.
2. Very good comparison between the two different techniques in several convection indices is noticed, in general, particularly in the trends though some difference exists in the amplitudes.
3. In general, for about 25% of time the EL is above 300 hPa revealing that MWR observations are not good enough to estimate the CAPE over Gadanki region. EL is above 300 hPa for about 24.9%, 39.5%, 35.1% and 4% during pre-monsoon, monsoon, post-monsoon and winter, respectively.
4. Strong diurnal variation in all the stability indices is noticed with maximum during 1400 h–1700 h LT where the maximum convection is expected to take place at this station and minimum during mid-night hours to early morning hours. Strong day-to-day variations in all the stability indices are noticed within afternoon hours.
5. Reasonably good comparison is seen in MUCAPE between the radiosonde and MWR estimated values. However, the maximum difference between the radiosonde and MWR can go as high as 60% during morning hours. Interestingly

during peak convection time (1400–1700 h LT) the error between the two estimates is minimum.

6. Large diurnal variation in the convection indices is observed in all the seasons except in winter over this tropical station.

We strongly believe that this information is very much useful when assimilating MWR data in models for Nowcasting whenever frequent radiosonde observations are unavailable. Similar analysis has also done by Madhulatha et al. (in press) at our location and found good comparison between thermodynamic parameters derived from MWR and co-located GPS radiosonde observations, indicating that MWR observations can be used for developing techniques for now-casting severe convective activity.

Acknowledgments

We acknowledge the Advanced Centre for Atmospheric Science funded by the Department of Space (DOS) under RESPOND to S. V. University, Tirupati, and Department of Science and Technology (DST) for providing fellowship to D.S. and also the necessary facilities to carry out this work. Intensive radiosonde campaign is conducted as part of CAWSES India Phase-II Programme fully funded by Department of Space (DOS). We thank all the three anonymous reviewers for their critical comments/suggestions which made to improve the manuscript to its present form.

References

Cady-Pereira, K.E., Shephard, M.W., Turner, D.D., Mlawer, E.J., Clough, S.A., Wagner, T.J., 2008. Improved daytime column-integrated precipitable water vapor from Väisälä radiosonde humidity sensors. J. Atmos. Ocean. Technol. 25, 873–883 http://dx.doi.org/10.1175/2007JTECHA1027.1.

Chan, P.W., 2009. Performance and application of a multi-wavelength, ground based microwave radiometer in rain nowcasting. Meteorol. Z. 18, 253–265.

Chan, P.W., Hon, K.K., 2011. Application of ground-based, multi-channel microwave radiometer in the nowcasting of intense convective weather through instability indices of the atmosphere. Meteorol. Z. 20 (4), 431–440.

Cimini, D., Campos, E., Ware, R., Albers, S., Graziano, G., Oreamuno, J., Joe, P., Koch, S., Cober, S., Westwater, E., 2011. Thermodynamic atmospheric profiling during the 2010 Winter Olympics using ground-based microwave radiometry. IEEE Trans. Geosci. Remote. Sens. 49 (12), 4959–4969.

Cimini, D., Dupont, J., Haeffelin, M., Angelis, F.D., 2012. Mixing height retrievals by microwave multichannel observations: potential for instrument synergy. 16th International Symposium for the Advancement of Boundary-Layer Remote Sensing, Boulder, Colorado, USA.

Dai, A., 2000. Global precipitation and thunderstorm frequencies. Part II: Diurnal variations. J. Clim. 14, 1112–1118.

Dhaka, S.K., Sapra, R., Panwar, V., Goel, A., Bhatnagar, R., Kaur, M., 2010. Influence of large-scale variations in convective available potential energy (CAPE) and solar cycle over temperature in the tropopause region at Delhi (28.3°N, 77.1°E), Kolkata (22.3°N, 88.2°E), Cochin (10°N, 77°E), and Trivandrum (8.5°N, 77.0°E) using radiosonde during 1980–2005. Earth Planets Space 62 (3), 319–331 http://dx.doi.org/10.5047/eps.2009.09.001.

George, J.J., 1960. Weather Forecasting for Aeronautics. Academic Press, New York.

Gettelman, A., Seidel, D.J., Wheeler, M.C., Ross, R.J., 2002. Multidecadal trends in tropical convective available potential energy. J. Geophys. Res. 107 (D21), 4606 http://dx.doi.org/10.1029/2001JD001082.

Gray, W.M., Jacobson, R.W., 1977. Diurnal variation of deep cumulus convection. Mon. Weather Rev. 105 (9), 1171–1188.

Herzegh, P., Landolt, S., Schneider, T., 2004. The structure, evolution and cloud processes of a colorado upslope storm as shown by profiling radiometer, radar and tower data. Proc. 31st Conf. on Radar Meteor., Amer. Met. Soc, Seattle, WA.

Johnson, R.H., Ciesielski, P.E., Lecuyer, T.S., Newman, A.J., 2010. Diurnal cycle of convection during the 2004 North American Monsoon Experiment. J. Clim. 23, 1060–1078.

Knupp, K., Ware, R., Cimini, D., Vandenberghe, F., Vivekanandan, J., Westwater, E., Coleman, T., 2009. Ground-based passive microwave profiling during dynamic weather conditions. J. Atmos. Ocean. Technol. http://dx.doi.org/10.1175/2008JTECHA1150.1.

Kottayil, A., Buehler, S.A., John, V.O., Miloshevich, L.M., Milz, M., Holl, G., 2011. On the importance of Vaisala RS92 radiosonde humidity corrections for a better agreement between measured and modeled satellite radiances. J. Atmos. Ocean. Technol. http://dx.doi.org/10.1175/JTECH-D-11-00080.1.

Madhulatha, A., Rajeevan, M., Venkat Ratnam, M., Jyoti Bhate, Naidu, C.V., in press. Nowcasting severe convective activity over South-east India using ground-based microwave radiometer observations. J. Geophys. Res. http://dx.doi.org/10.1029/2012JD018174.

Mattioli, V., Westwater, E.R., Cimini, D., Liljegren, J.C., Lesht, B.M., Gutman, S.I., Schmidlin, F.J., 2007. Analysis of radiosonde and ground-based remotely sensed PWV data from the 2004 North Slope of Alaska Arctic Winter Radiometric Experiment. J. Atmos. Ocean. Technol. http://dx.doi.org/10.1175/JTECH1982.1.

Mc Garry, M.M., Reed, R.J., 1977. Diurnal variation in convective activity and precipitation during phases II and III of GATE. Mon. Weather Rev. 106, 101–103.

Miller, R.C., 1967. Notes on analysis and severe storm forecasting procedures of the Military Weather Warning Center. Tech. Report. 200, AWS, USAF.

Miloshevich, L.M., Vomel, H., Paukkunen, A., Heymsfield, A.J., Oltmans, S.J., 2001. Characterization and correction of relative humidity measurements from Vaisala RS80-A radiosondes at cold temperatures. J. Atmos. Ocean. Technol. 18, 135–156.

Miloshevich, L.M., Paukkunen, A., Vomel, H., Oltmans, S.J., 2004. Development and validation of a time-lag correction for Väisälä radiosonde humidity measurements. J. Atmos. Ocean. Technol. 21, 1305–1327 http://dx.doi.org/10.1175/1520-0426(2004)021<1305:DAVOAT>2.0.CO;2.

Miloshevich, L.M., Vomel, H., Whiteman, D.N., Lesht, B.M., Schmidlin, F.J., Russo, F., 2006. Absolute accuracy of water vapor measurements from six operational radiosonde types launched during AWEX-G, and implications for AIRS validation. J. Geophys. Res. 111 (D09S10) http://dx.doi.org/10.1029/2005JD006083.

Miloshevich, L.M., Vömel, H., Whiteman, D.N., Leblanc, T., 2009. Accuracy assessment and correction of Vaisala RS92 radiosonde water vapor measurements. J. Geophys. Res. 114, D11305 http://dx.doi.org/10.1029/2008JD011565.

Monkam, David, 2002. Convective Available Potential Energy (CAPE) in North Africa and Tropical Atlantic and study of its connections with rainfall in central and West Africa during summer 1985. Atmos. Res. 62, 125–147.

Narendra babu, A., Nee, J.B., Kishore Kumar, K., 2009. Seasonal and diurnal variation of convective available potential energy (CAPE) using COSMIC/FORMOSAT-3 observations over the tropics. J. Geophys. Res. 115 (D04102) http://dx.doi.org/10.1029/2009JD012535.

Peppler, R.A., Lamb, P.J., 1989. Tropospheric static stability and Central North American growing season rainfall. Mon. Weather Rev. 117, 1156–1180.

Rowe, M.P., Miloshevich, L.M., Turner, D.D., Walden, V.P., 2008. Dry bias in Vaisala RS90 radiosonde humidity profiles over Antarctica. J. Atmos. Ocean. Technol. 25, 1529–1541.

Sanchez, J.L., Posada, R., Garcıa-Ortega, E., Lopez, L., Marcos, J.L., 2012. A method to improve the accuracy of continuous measuring of vertical profiles of temperature and water vapor density by means of a ground-based microwave radiometer. Atmos. Res. http://dx.doi.org/10.1016/j.atmosres.2012.10.024.

Sapra, R., Dhaka, S.K., Panwar, V., Bhatnagar, R., Praveen Kumar, K., Shibagaki, Y., Venkat Ratnam, M., Takahashi, M., 2011. Long-term variations in outgoing long-wave radiation (OLR), convective available potential energy (CAPE) and temperature in the tropopause region over India. J. Earth Syst. Sci. 120 (5), 807–823.

Sato, T., Kimura, F., 2004. Diurnal cycle of convective instability around the central mountains in Japan during the warm season. J. Atmos. Sci. 62, 1626–1636.

Soden, B.J., 2000. Diurnal variation of convection, clouds, and water vapor in the tropical upper troposphere. Geophys. Res. Lett. 27, 2173–2176.

Sui, C.H., Lau, K.M., Takayabu, Y.M., Short, D.A., 1997. Diurnal variations in tropical oceanic cumulus convection during TOGA COARE. J. Atmos. Sci. 54, 639–655 http://dx.doi.org/10.1175/1520-0469(1997.

Turner, D.D., Lesht, B.M., Clough, S.A., Liljegren, J.C., Revercomb, H.E., Tobin, D.C., 2003. Dry bias and variability in Vaisala RS80-H radiosondes: the ARM experience. J. Atmos. Ocean. Technol. 20, 117–132 http://dx.doi.org/10.1175/1520-0426(2003)020<0117:DBAVIV>2.0.CO;2.

Ueno, K., Aryal, R., 2007. Impact of tropical convective activity on monthly temperature variability during nonmonsoon season in the Nepal Himalayas. J. Geophys. Res. 113, D18112 http://dx.doi.org/10.1029/2007JD0095242008.

Vandenberghe, F., Ware, R., 2002. 4-Dimensional variational assimilation of ground-based microwave observations during a winter fog event. International Workshop on GPS Meteorology, Tsukuba, Japan.

Ware, R., Cimini, D., Giuliani, G., Campos, E., Oreamuno, J., Joe, P., Cober, S., Albers, S., Koch, S., Westwater, E., 2010. Thermodynamic profiling at the Alpine Venue of the 2010 Winter Olympics. WMO Technical Conference on Meteorological and Environmental Instruments and Methods of Observation (TECO −2010), Helsinki, Finland.

Westwater, E.R., 1997. Remote sensing of tropospheric temperature and moisture by integrated observing systems. Bull. Am. Meteorol. Soc. 78, 1991–2006.

Westwater, E.R., Boba Stankov, B., Cimini, D., Han, Y., Joseph, A., Lesht, B.M., Long, C.N., 2003. Radiosonde humidity soundings and microwave radiometers during Nauru99. J. Atmos. Ocean. Technol. 20, 953–971.

Zhang, G.J., 2003. Diurnal cycle of convection at the ARM SGP site: role of large-scale forcing, surface fluxes, and convective inhibition. Thirteenth ARM Science Team Meeting Proceedings, Broomfield, Colorado.